

ON THE “INDUCTION BIAS” IN SEQUENCE MODELS

Anonymous authors

Paper under double-blind review

ABSTRACT

Despite the remarkable practical success of transformer-based language models, recent work has raised concerns about their ability to perform state tracking. In particular, a growing body of literature has shown this limitation primarily through failures in out-of-distribution (OOD) generalization, such as length extrapolation. In this work, we shift attention to the in-distribution implications of these limitations. We empirically compare the data efficiency of transformers and recurrent neural networks (RNNs) across multiple supervision regimes. We find that the amount of training data required by transformers grows much more rapidly with state-space size and sequence length than for RNNs. Furthermore, we analyze the extent to which learned state-tracking mechanisms are shared across different sequence lengths. We show that transformers exhibit negligible or even detrimental weight sharing across lengths, indicating that they learn length-specific solutions in isolation. In contrast, recurrent models exhibit effective amortized learning by sharing weights across lengths, allowing data from one sequence length to improve performance on others. Together, these results demonstrate that state tracking remains a fundamental challenge for transformers, even when training and evaluation distributions match.

1 INTRODUCTION

State tracking is a key capability of most intelligent systems and of most models of computation. It is the process of monitoring and updating the status of an entity or process with which the system interacts over a period of time. State tracking is particularly important in multi-hop, interactive tasks, such as that of an agent interacting with an interface or of a dialogue system interacting with a user across multiple turns.

State tracking has become a popular area of investigation in recent years, especially in the study of LLM capabilities and failure modes. In this context, numerous studies have shown that transformer-based models are fundamentally limited in their ability to perform state tracking (for example, (Anil et al., 2022a; Dziri et al., 2024)). This contrasts with recurrent networks, which excel at state tracking (although their wide-spread applicability is unfortunately hampered by their relative training inefficiency). The limitations of transformers have been demonstrated as limitations in out-of-distribution (OOD) generalization, specifically length-generalization: after training models on tasks encoded in sequences of a given range of lengths, they were evaluated on sequences with lengths that were not seen during training. In these scenarios, the trained models fail to consistently generate correct outputs on the evaluation data, although they are able to solve the tasks for even unseen sequences in the training range of lengths.

It could be argued that in any real-world use-cases, OOD state tracking failures may not be an issue as long as enough training data with step-by-step sequential supervision is available. If training data covers all sequence lengths that may be encountered at inference time, inference can rely entirely on in-distribution generalization. Unfortunately, although this argument is true in principle, it is hard to quantify “enough” in this context. It is also hard to quantify how the amount of training data required for any given task may depend on the length of the sequences and the size of the state space.

To shed light onto these questions, in this work we perform a detailed and systematic empirical study of the *in-distribution* performance of transformer-based models and contrast these with recurrent models. To this end, we train and evaluate a range of representative models on a range of simple state tracking tasks. Independently varying sequence length and size of the state space in these tasks then

allows us to discover regularities in the dependence of generalization error on these parameters. This in turn makes it possible to obtain a crude “lower bound” of the minimal amount of training data likely required to solve such tasks.

A key difference between transformer-based and recurrent models is that, at every timestep, the former compute outputs by applying a function that depends on *all* inputs and outputs generated previously (the context window), making it possible, in principle, to re-calculate the required state from the past information globally at each time step. Recurrent networks, on the other hand, compute outputs by applying a function that depends on only the current hidden state, making it impossible to perform such a re-calculation. This makes it strictly necessary for a recurrent network to encode any relevant information from the past within a single hidden state vector. This inductive bias encourages a recurrent network to incorporate the information from the current timestep into its representation of state at the moment where this information is available. Conversely, it discourages it from “saving” this information off to determine future state updates globally from the past information. The immediate state updates thus encourage the network to process the input sequence step-by-step, making any state update explicit as soon as this is possible, rather than potentially deferring such updates to a later point in time.

Such step-by-step state updates are a natural inductive bias (Mitchell, 1997) in the context of simple state tracking tasks, as they make it possible to reduce complex multi-step dependencies to a sequence of single-step computations. They also allow a model to share weights across multiple different sequence lengths, as it breaks state updates into single-step, repeatable computations. By analogy to the induction step in a mathematical proof, we shall refer to this kind of inductive bias in this work as “induction bias” (sic). We show that the presence (or respectively absence) of an induction bias, or its relative strength, provides a simple explanation for a wide range of the empirical findings we present.

Key take-aways from our study include the following:

- We show that there is a distinct difference between the supervision regimes in which transformers and recurrent networks perform well in-distribution.
- We show that transformers can relatively efficiently learn state tracking tasks in-distribution on one (fixed) sequence length at a time, but generalizing in-distribution over multiple sequence lengths requires significantly more training data.
- We present evidence that, unlike recurrent networks, transformers tend to fail at sharing parameters across sequence lengths and instead learn separate solution mechanisms for different lengths.
- We show that the degree of knowledge transfer across multiple different sequence lengths in the in-distribution setting is highly correlated with the ability of a model to length-generalize.

Related work A range of studies has shown that transformer-based sequence models fail to length-generalize in state tracking tasks (Anil et al., 2022b; Deletang et al., 2023; Dziri et al., 2024; Abbe et al., 2024; Ebrahimi et al., 2024). Unlike our work, these studies solely discuss OOD scenarios, while we discuss in-distribution data efficiency instead.

The inability to length-generalize in state tracking tasks has been shown to hold also for most existing state-space models (SSM) (Sarraf et al., 2024; Merrill et al., 2024). However recent work has shown that making the hidden-to-hidden transition matrix in the SSM input-dependent and non-diagonal can recover the ability to length-generalize. (Fan et al., 2024; Grazzi et al., 2025; Ebrahimi & Memisevic, 2025; Beck et al., 2024).

Finally, Liu et al. (2023) and Li et al. (2025) show that transformers solve state tracking tasks in-distribution by making use of parallel mechanisms reminiscent of associative scan. While this view can help explain the OOD failures of these models, it also hints at the absence of an “induction” bias which affects data efficiency as we show in this work.

2 METHODOLOGY

Task: We consider the task of modular addition, where a model is provided a sequence of n integers $\mathbf{x} = (x_1, x_2, \dots, x_n)$ with each x_i drawn uniformly at random from $\mathbb{Z}_m = \{0, 1, \dots, m - 1\}$. The

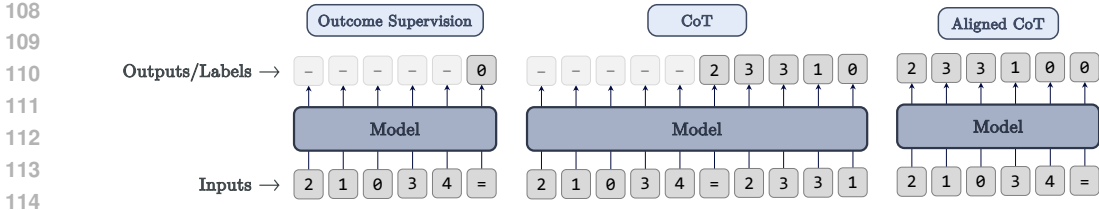


Figure 1: Example of the three task formats for the addition modulo 5 task applied to the sequence 21034.

objective is to compute the sum of the sequence modulo m :

$$y = \left(\sum_{i=1}^n x_i \right) \pmod{m}, \quad x_i \in \mathbb{Z}_m.$$

For $m = 2$, the task reduces to computing the parity of a binary sequence. From an algebraic perspective, modular addition over \mathbb{Z}_m (cyclic group) serves as the canonical representative for commutative operations, as every finite abelian group is isomorphic to a direct product of such cyclic groups.

We also experiment with non-commutative operations by considering the task of permutation composition over the symmetric group S_5 . This task serves as the canonical non-commutative counterpart for state tracking, as by Cayley’s Theorem, every finite group is isomorphic to a subgroup of a symmetric group (Dummit et al., 2004). For additional details and empirical results on the permutation composition task, we refer the reader to Appendix Section B.2.

Length Distributions: For each generated sample, we first determine the sequence length $n \in \{2, \dots, L\}$, where L denotes the maximum sequence length. We then sample a sequence $\mathbf{x} \in \mathbb{Z}_m^n$ without replacement to ensure that every sample in the dataset is unique. We use three distinct strategies for length selection:

1. *Fixed:* The length is held constant at $n = L$.
2. *Uniform:* Lengths are sampled uniformly at random from the set $\{2, \dots, L\}$.
3. *Short-to-Long:* Sequences are sampled in ascending order of length, exhausting the available sequences for length n before proceeding to $n + 1$.

Task Formats: We consider three task formats that vary in the density and structure of the supervision signal. Let $s_k = (\sum_{i=1}^k x_i) \pmod{m}$ denote the k -th partial sum of the input sequence. The formats, illustrated in Figure 1, are defined as follows:

1. *Outcome Supervision:* The model is provided the input sequence \mathbf{x} and is trained to predict only the final sum s_n . This format provides no intermediate supervision, requiring the model to discover the latent computational logic of the task on its own during training.
2. *Chain-of-Thought (CoT):* The model is trained to generate the sequence of intermediate partial sums (s_1, s_2, \dots, s_n) following the input sequence. This decomposes the task into a sequence of iterative applications of the operator.
3. *Aligned Chain-of-Thought (ACoT):* The model is tasked to output, for each input token x_i , the corresponding partial sum s_i . While conceptually similar to the scratchpad, this format provides per-token supervision that is aligned with the input. This format is similarly used in prior work (Li et al., 2025; Zhang et al., 2025) and is also referred to as *state-supervision*.

Unlike outcome supervision, both CoT and ACoT constitute a form of *process supervision*, as they provide explicit training signals for the intermediate solution steps.

Sample Efficiency: To quantify the data efficiency of a model under a specific task configuration, we define the *minimal sample size* N^* required to learn the task reliably. Let \mathcal{D}_N denote a training set of cardinality N , and let $\mathcal{L}_{\text{val}}(\phi; \mathcal{D}_N)$ denote the validation loss of a model trained on \mathcal{D}_N using hyperparameter configuration $\phi \in \Phi$.

We consider a task successfully learned if the minimum validation loss over the hyperparameter grid falls below a convergence threshold:

$$\min_{\phi \in \Phi} \mathcal{L}_{\text{val}}(\phi; \mathcal{D}_N) \leq \epsilon, \quad (1)$$

where Φ is a predefined grid of learning rates and random seeds, and ϵ is a convergence threshold. Formally, we define N^* as the smallest training set size satisfying this criterion:

$$N^* = \min \left\{ N \in \mathbb{N} : \min_{\phi \in \Phi} \mathcal{L}_{\text{val}}(\phi; \mathcal{D}_N) \leq \epsilon \right\}. \quad (2)$$

In practice, we estimate N^* by performing a binary search over the training set size. Note that both training and validation samples are drawn from the same underlying data generation process, and therefore N^* reflects the *in-distribution* sample efficiency. In addition to low validation loss, we also consider perfect validation accuracy as an alternative success criterion and find no meaningful difference in the results. For the results in Section 4, we use the latter.

Models: We compare multi-layer decoder-only transformer architecture (Vaswani et al., 2017), with two recurrent alternatives: Long Short-Term Memory (LSTM) (Hochreiter & Schmidhuber, 1997) and dense state-space models (Dense-SSMs) (Fan et al., 2024; Terzić et al., 2025; Ebrahimi & Memisevic, 2025).

In Dense-SSMs, the state transition matrix is dense and fully input-dependent, a property shown to support effective state tracking in linear recurrent models (Merrill et al., 2024; Terzić et al., 2025). We adopt the variant used by Ebrahimi & Memisevic (2025), in which input–state interactions are purely multiplicative and the state update has no additive term:

$$h_t = A_{x_t} h_{t-1}, \quad (3)$$

where the transition matrix A_{x_t} is given by a linear function of the input x_t . This architecture is commonly referred to as a *bilinear RNN*, since h_t depends bilinearly on the input and the previous hidden state.

Experimental Setup: We perform a large-scale systematic evaluation of data efficiency on synthetic state-tracking tasks. To estimate N^* , we use a hybrid binary–geometric search procedure (see Algorithm 1) that evaluates candidate sample sizes over at most 20 steps, training models across a hyperparameter grid consisting of 3 learning rates and 5 random seeds (15 configurations total for each size N). A sample size is considered successful if at least one configuration achieves validation loss below $\epsilon = 10^{-4}$. Each model is trained for a fixed budget of 250k optimization steps independent of the training set size N . This amounts to over *190,000 training runs* for the results reported in this paper, excluding development runs.

The transformer model used is based on the GPT-2 architecture (Radford et al., 2019) with 6 layers and a model (embedding/hidden) dimension of 256. Both the LSTM and Dense-SSM models use a single-layer recurrent cell followed by a linear classification head. We use input and hidden dimension of 768 for LSTM and 256 for the Dense-SSM. Additionally, we experiment with a 2-layer transformer and LSTM with hidden dimension of 256, with sample efficiency results provided in the Appendix Section B.3.

We ensure that the training and validation sets are strictly disjoint. The validation set contains 2,000 samples (or at most 20% of the available data) and remains identical across different training set sizes, except for variations introduced by the random seed. In addition, we always use at most 20% of the available samples at each sequence length for validation, with the remainder reserved exclusively for training. Also, for all tasks, multi-digit integers are represented as single tokens during tokenization. Finally, for the Chain-of-Thought task format, validation loss is computed using teacher forcing rather than autoregressive sampling. Additional implementation details are provided in Appendix A.

3 IN-DISTRIBUTION DATA EFFICIENCY

We perform the above binary search procedure to identify the minimal dataset size (N^*) across all combinations of maximum sequence length $L \in \{5, 10, 20, 30\}$ and modulus $m \in \{2, 3, 5, 10, 15, 20, 50, 75, 100\}$, for each of the three task formats, length distributions, and models

216 described earlier. The results are summarized in Table 1. For ease of comparison, we also visualize
 217 selected slices of this table in figures throughout this section. Comparable results for models of
 218 different sizes are reported in Appendix Section B.3. From the table we can infer the following key
 219 observations:

220 **Observation 3.1.** *Transformers prefer non-aligned supervision (Chain of Thought).*

221 We observe a clear preference of transformers
 222 for CoT over the Aligned CoT format. For exam-
 223 ple, at $m = 5$ and $L = 20$, CoT requires
 224 1.7K samples, while Aligned CoT requires 2M,
 225 an order-of-magnitude increase in sample com-
 226 plexity. Figure 2 further illustrates this gap in
 227 sample requirements for the case $m = 2$ (parity)
 228 across the two formats.

229 It has been hypothesized that by outputting in-
 230 termediate steps autoregressively, the model
 231 can attend to its own previous outputs, effec-
 232 tively simulating a larger depth circuit (Li et al.,
 233 2024), and the results confirm this hypothesis.
 234 In contrast, Aligned Chain-of-Thought forces
 235 the model to compress the computation into a
 236 single forward pass per token without the bene-
 237 fit of re-attending to intermediate results, which
 238 appears less aligned with the transformer’s non-
 239 recurrent nature.

240 **Observation 3.2.** *Recurrent models prefer aligned supervision (Aligned Chain-of-Thought).*

241 Conversely, recurrent models (LSTMs and Dense-SSMs) demonstrate superior sample efficiency
 242 when trained with the Aligned CoT (ACoT) format, which provides supervision aligned with the
 243 evolution of the hidden state (see also Figure 2).

244 In contrast, RNNs struggle with CoT, which is likely due to their recall bottleneck (Wen et al.,
 245 2025): a model must output the sequence of partial sums (s_1, \dots, s_n) after processing the entire
 246 input sequence. This effectively requires it to unroll the chain of intermediate computations from
 247 the beginning. In fact, we note that under the CoT format, recurrent models even fail to generalize
 248 to longer sequences despite their sequential inductive bias (see Table 2 for length-generalization
 249 results). The task thereby becomes bottlenecked by the model’s limited memory capacity rather than
 250 its state-tracking ability.

251 **Observation 3.3.** *Recurrent models outperform transformers in the absence of intermediate supervi-
 252 sion.*

253 In the Outcome Supervision setting, the model
 254 must implicitly infer the latent algebraic struc-
 255 ture of the task solely from the final solution,
 256 without any guidance on the intermediate steps.
 257 This requires the model to effectively marginal-
 258 ize over unobserved computational paths with
 259 difficulty scaling with both the state space size
 260 m and sequence length n .

261 We observe that recurrent models significantly
 262 outperform transformers in this regime. While
 263 transformers fail to converge for all but the
 264 most trivial configurations (very small m and
 265 n), the recurrent architectures successfully learn
 266 the task for higher moduli and extended se-
 267 quence lengths, achieving convergence with or-
 268 ders of magnitude fewer training samples. Fig-
 269 ure 3 illustrates this behavior for the parity case
 ($m = 2$).

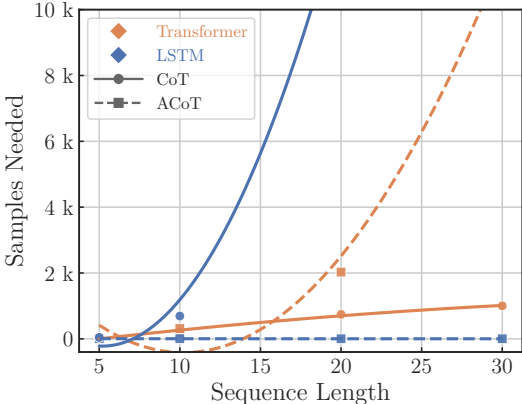


Figure 2: Minimal dataset size for the uniform length distribution with $m = 2$ (parity). RNNs favor ACoT, whereas transformers favor CoT.

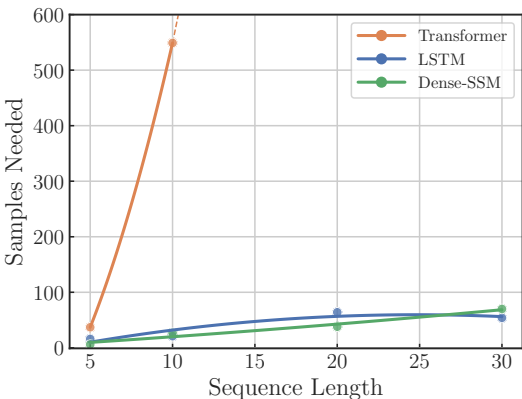


Figure 3: N^* for the outcome supervision format with a uniform length distribution and $m = 2$ (parity). In the absence of intermediate supervision, single-layer RNNs significantly outperform the 6-layer transformer.

Observation 3.4. *With intermediate supervision, longer sequences improve the data efficiency of recurrent models but not transformers.*

Intuitively, under formats with intermediate supervision (CoT or ACoT), longer sequences should improve sample efficiency. This is because with intermediate solutions, the effective amount of supervised tokens increases linearly with sequence length.

We validate this hypothesis in recurrent models trained with Aligned Chain-of-Thought: the fixed length distribution (comprising only longest sequences) yields the highest data efficiency, followed by uniform, and finally short-to-long.

Furthermore, in the uniform setting, we find that recurrent models trained with ACoT require fewer data points as the maximum sequence length L increases, as expected. In contrast, transformers trained with CoT fail to leverage this additional supervision. This trend is also evident in Figure 4, which compares sample complexity on the parity task.

Observation 3.5. *With outcome supervision, short sequences are more valuable for recurrent models.*

In the Outcome Supervision setting, we compare the data requirements under the uniform and short-to-long length distributions. Recall that these two distributions differ only in the order in which samples are presented during training.

We observe that recurrent models require fewer samples in the short-to-long setting, suggesting that shorter sequences provide a stronger learning signal than longer sequences for these models. This effect is illustrated in Figure 5 for the case $m = 2$.

Altogether, these observations provide evidence that the key difference enabling data efficiency for recurrent networks, and even more so the Dense-SSM models, is their tendency to represent state transitions inherent in the data generation process at every time-step.

4 WEIGHT SHARING ACROSS SEQUENCE LENGTH

A key hypothesis for why recurrent networks dominate transformers with respect to data efficiency, as shown in the previous section, is that their “induction bias” encourages step-by-step updates to their representations of state. This, in turn, should allow the model to share the same solution mechanisms across the whole sequence length.

In this section, we investigate the extent to which the learned mechanisms are shared across different sequence lengths. Specifically, we examine whether the model develops length-specific heuristics, effectively “specialized circuits” for fixed-length sequences, or whether it has internalized the inherent inductive structure of the task. The latter implies the discovery of a transition operator that can be applied iteratively. Assessing the degree of this cross-length sharing is critical for understanding a model’s inductive capacity and to generalize to sequence lengths not encountered in the training distribution.

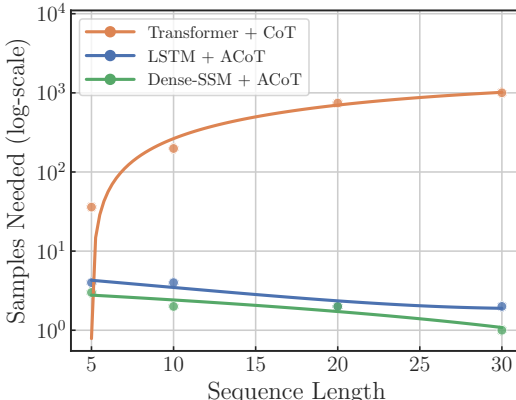


Figure 4: Sample complexity (log scale) for transformers trained with CoT and RNNs trained with ACoT on the parity task. RNNs exhibit the expected improvement in sample efficiency with increasing sequence length, while transformers fail to leverage the additional supervision.

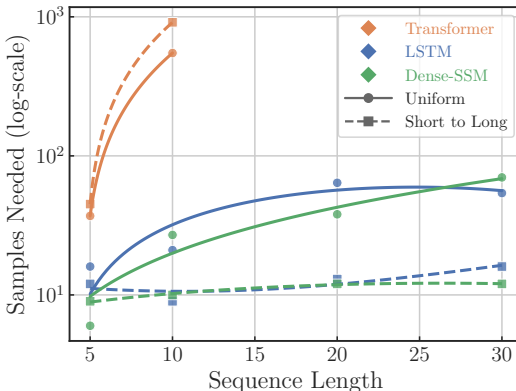


Figure 5: Sample complexity (log scale) in the Outcome Supervision format for the uniform and short-to-long settings, with $m = 2$.

Table 1: Minimal number of training samples required to learn the modulo addition task. A dash (–) indicates that the task was not learned at the maximum training set size.

Model	Format	Mod.	Fixed				Uniform				Short-to-Long			
			5	10	20	30	5	10	20	30	5	10	20	30
Transformer	Outcome Supervision	2	19	364	–	–	37	549	–	–	45	913	–	–
		3	119	–	–	–	–	–	–	–	243	–	–	–
		5	1.1K	–	–	–	2.6K	–	–	–	1.5K	–	–	–
		10	–	–	–	–	–	–	–	–	–	–	–	–
		15	–	–	–	–	–	–	–	–	–	–	–	–
		20	–	–	–	–	–	–	–	–	–	–	–	–
		50	–	–	–	–	–	–	–	–	–	–	–	–
		75	–	–	–	–	–	–	–	–	–	–	–	–
		100	–	–	–	–	–	–	–	–	–	–	–	–
		Transformer	CoT	2	10	16	19	20	36	198	744	1K	39	824
3	16			18	21	25	78	465	1.2K	1.4K	108	28.8K	–	–
5	33			30	31	34	148	1.1K	1.7K	1.7K	647	2.4M	–	–
10	94			66	62	70	427	2.3K	3.4K	4K	11K	–	–	–
15	166			116	78	107	709	2.5K	5K	5.1K	54.3K	–	–	–
20	377			178	116	135	1K	3.8K	5.6K	7.4K	168.6K	–	–	–
50	1.1K			678	553	470	2.6K	8.6K	12K	11.2K	6.4M	–	–	–
75	1.7K			1.2K	1K	946	4.2K	11K	18.1K	16.1K	–	–	–	–
100	2.5K			1.9K	1.6K	1.6K	5.8K	13.2K	21.1K	19.1K	–	–	–	–
Transformer	Aligned CoT			2	16	121	644	1.2K	27	313	2K	11.7K	19	856
		3	91	2K	3.7K	4K	180	8.3K	66.8K	–	207	29.7K	–	–
		5	528	3.9K	9.2K	20.8K	671	14.5K	2M	–	909	2.4M	–	–
		10	1.3K	6K	15.5K	131.4K	1.7K	32.3K	–	–	11.2K	–	–	–
		15	1.5K	7.9K	23.3K	–	2.4K	61.5K	–	–	55K	–	–	–
		20	2.6K	21.9K	85.3K	–	4.5K	190.9K	–	–	172.6K	–	–	–
		50	13K	1M	–	–	22K	–	–	–	6.7M	–	–	–
		75	21.1K	15.2M	–	–	102.1K	–	–	–	–	–	–	–
		100	23.6K	–	–	–	8M	–	–	–	–	–	–	–
		LSTM	Outcome Supervision	2	14	101	252	309	16	21	64	54	12	9
3	195			620	1.7K	–	78	122	317	526	83	90	90	100
5	2K			5.9K	–	–	387	707	–	–	381	22.7K	–	–
10	6.4K			–	–	–	2.2K	8.6K	–	–	2.2K	–	–	–
15	18.8K			–	–	–	11.8K	–	–	–	–	–	–	–
20	–			–	–	–	–	–	–	–	–	–	–	–
50	–			–	–	–	–	–	–	–	–	–	–	–
75	–			–	–	–	–	–	–	–	–	–	–	–
100	–			–	–	–	–	–	–	–	–	–	–	–
LSTM	CoT			2	20	307	4.7K	8.6K	45	692	13.4K	37.1K	48	843
		3	–	2.9K	9.3K	14K	–	7.4K	40.3K	5.2M	–	29K	–	–
		5	1.6K	10.3K	20.4K	44K	2K	28.4K	68.1K	2.1M	2.1K	–	–	–
		10	6.1K	15.7K	29.1K	–	14.3K	544.4K	500K	–	16.8K	–	–	–
		15	15.8K	21.1K	42K	–	32K	67K	–	–	65.6K	–	–	–
		20	21.2K	29.6K	54.3K	–	40.7K	409.1K	14M	–	215.4K	–	–	–
		50	43K	50.4K	–	–	206K	2.2M	–	–	10.4M	–	–	–
		75	56.5K	58K	–	–	4M	–	–	–	–	–	–	–
		100	84.2K	9.5M	–	–	–	–	–	–	–	–	–	–
		Dense-SSM	Aligned CoT	2	4	6	2	2	4	4	2	2	9	7
3	10			8	8	6	18	12	6	8	27	28	34	34
5	95			70	39	31	153	107	80	47	142	148	253	235
10	278			194	146	130	447	313	247	232	685	1.3K	1.8K	2K
15	534			478	409	371	865	631	567	500	1.5K	3.9K	5.2K	7.1K
20	798			672	652	798	1.3K	934	870	820	2.7K	9.4K	13.4K	25.9K
50	3.7K			4.6K	6K	7.4K	4.1K	5.3K	6.1K	6.9K	14.7K	156.2K	–	–
75	7.4K			9.2K	12.2K	13.3K	8.4K	11.3K	14.2K	16.8K	41.1K	697.4K	–	–
100	12.8K			16.6K	21.9K	23.7K	13.3K	19.4K	24.3K	28.5K	99.7K	–	–	–
Dense-SSM	Outcome Supervision			2	13	58	33	70	6	27	38	70	9	10
		3	56	390	8K	2.2K	31	69	209	265	24	32	41	41
		5	323	3.8K	10.9M	–	118	285	1K	1.1K	69	83	132	163
		10	2.7K	8.3M	–	–	573	2.2K	4.5K	–	321	452	678	1.1K
		15	6.5K	–	–	–	1.6K	–	12.1K	–	970	1.4K	3.7K	3.8K
		20	15.7K	–	–	–	3K	–	–	–	2K	8.4K	8.8K	9K
		50	–	–	–	–	15.6K	–	–	–	11K	–	–	–
		75	–	–	–	–	–	–	–	–	–	–	–	–
		100	–	–	–	–	–	–	–	–	–	–	–	–
		Dense-SSM	CoT	2	–	172	2.1K	–	–	511	–	–	–	875
3	110			1K	–	–	216	6.2K	–	–	234	29.8K	–	–
5	538			5.9K	–	–	1.5K	19.5K	–	–	1.5K	2.4M	–	–
10	3.4K			–	–	–	12.5K	–	–	–	14.8K	–	–	–
15	12.6K			–	–	–	21.2K	–	–	–	56.2K	–	–	–
20	21.9K			–	–	–	–	–	–	–	2.5M	–	–	–
50	–			–	–	–	–	–	–	–	–	–	–	–
75	–			–	–	–	–	–	–	–	–	–	–	–
100	–			–	–	–	–	–	–	–	–	–	–	–
Dense-SSM	Aligned CoT			2	2	2	3	1	3	2	2	1	6	4
		3	4	6	4	4	7	6	4	4	9	11	10	10
		5	18	9	6	6	24	17	10	10	30	26	25	25
		10	109	41	21	17	148	74	56	27	102	101	101	101
		15	219	109	66	37	412	186	101	70	228	225	225	225
		20	438	233	124	78	633	382	241	116	396	397	405	405
		50	3.2K	1.7K	1.1K	874	4.5K	3.2K	2K	1.6K	2.5K	2.5K	2.5K	2.5K
		75	8.1K	4K	3.1K	2.1K	10.8K	6.8K	5.1K	3.8K	5.6K	5.6K	5.6K	5.6K
		100	12.5K	6K	4.3K	3K	16.1K	10.2K	6.7K	6K	10K	10K	12.8K	16.4K

We quantify the cross-length mechanism sharing through the lens of sample efficiency. Intuitively, if a model utilizes a shared mechanism (e.g., a transition operator) across varying lengths, the sample cost to learn the task over a distribution of lengths should be significantly lower than the sum of costs to learn each length individually. This is due to the *amortization* of the learning cost: the data required to learn the operation at length n simultaneously contributes to the model’s learning at length $n + k$.

Formally, we compare the total number of training examples required for a model to simultaneously learn the task for all sequence lengths $n \in \{2, \dots, L\}$ (the joint task) against the sum of samples required by $L - 1$ independent models, each optimized for a single fixed length. Let N_{joint}^* denote the minimal sample size required for the joint task, and N_n^* denote the minimal sample size for a model trained and evaluated exclusively on sequences of length n . We define the *Sharing Factor* κ as:

$$\kappa = \frac{\sum_{n=2}^L N_n^*}{N_{\text{joint}}^*} \tag{4}$$

The value of κ provides insight into the extent of across-length mechanism sharing:

- $\kappa > 1$ indicates mechanism sharing and amortized learning. This suggests the model has internalized the inductive nature of the task, and data from one sequence length accelerates the acquisition of the task across the entire distribution.
- $\kappa \approx 1$ suggests that the model learns length-specific solutions in isolation, effectively partitioning capacity into independent circuits.
- $\kappa < 1$ represents a regime of destructive interference. In this case, the length-specific solutions compete for model capacity, making it more data-efficient to train separate models for each length than to optimize a single model for the joint task.

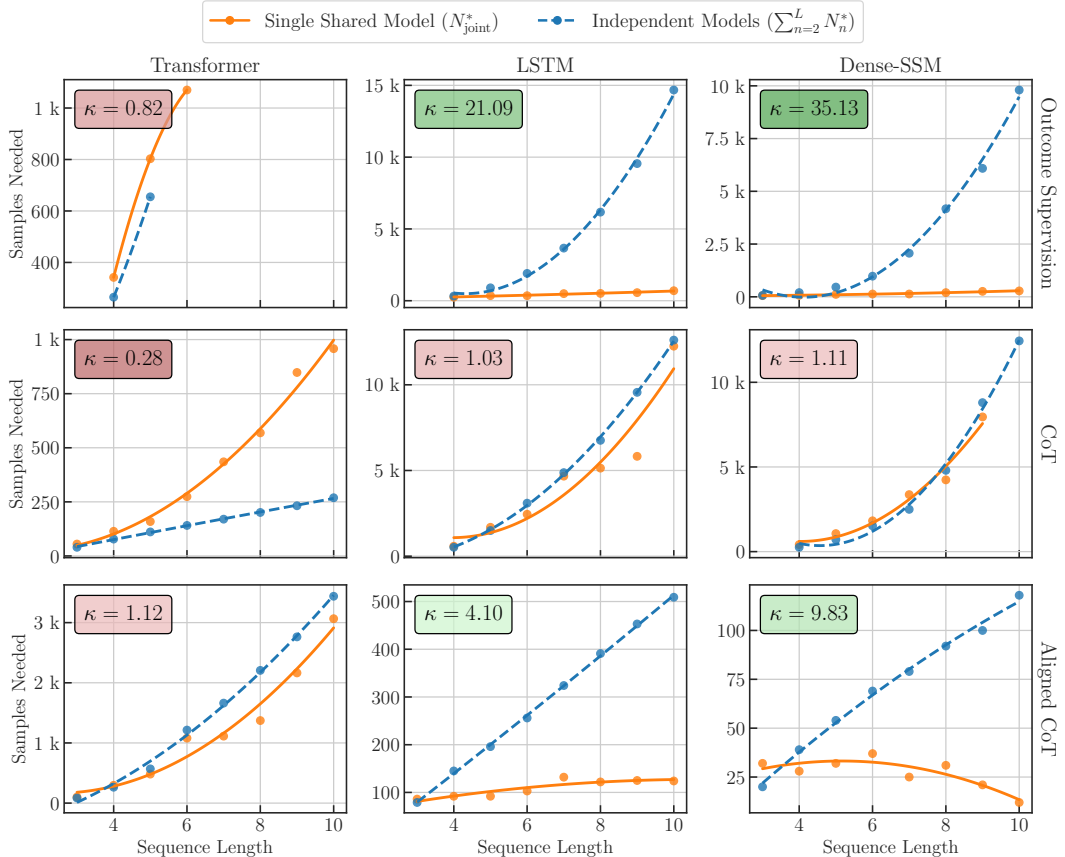


Figure 6: Sample complexity comparison between training a single model jointly across all sequence lengths and the cumulative sample complexity of independently trained models for each sequence length, together with the corresponding sharing factor. The results suggest that transformers learn largely isolated solutions for each sequence length.

Figure 6 illustrates the sample complexity to learn the task for all sequence lengths (N_{joint}^*) compared against the cumulative samples required by independent models trained on individual sequence lengths ($\sum_{n=2}^L N_n^*$), for $L \in \{2, \dots, 10\}$. We evaluate these metrics for modular addition with $m = 5$ across the three previously defined task formats, and draw the following key observations. Comparable results for the permutation composition task (symmetric group S_5) are reported in Appendix Section B.2.

Observation 4.1. *Transformers have low sharing factor for all task formats.*

As demonstrated, we observe a low sharing factor in transformers across all task formats, with $\kappa \approx 1$ or $\kappa < 1$ in all cases. Notably, in the Chain-of-Thought (CoT) setting, despite being transformer’s most efficient task configuration, we observe an extreme case of length isolation ($\kappa = 0.28$).

Observation 4.2. *Transformers show destructive interference with CoT.*

The observed sharing factor of $\kappa \ll 1$ for transformer with CoT indicates a regime of destructive interference where length-specific solutions compete for model capacity, such that training on a diverse length distribution is substantially less data-efficient than training independent models on each length.

Observation 4.3. *Recurrent networks have high sharing factors in their preferred task formats.*

In contrast, both recurrent models exhibit clear evidence of mechanism sharing and amortized learning across sequence lengths ($\kappa \gg 1$) under the Outcome Supervision and Aligned Chain-of-Thought formats. However, this is no longer the case in the Chain-of-Thought format ($\kappa \approx 1$), where the recurrent models also fail to share across the sequence lengths, likely due to the previously discussed recall bottleneck. However, unlike transformers, we do not observe destructive interference in this case.

Observation 4.4. *Longer sequences increase data efficiency for Dense-SSMs.*

As noted in the previous section, the sample requirement for the Dense-SSM under ACoT *decreases* as the maximum sequence length L increases. This indicates that through cross-length mechanism sharing, the model leverages the higher density of supervision signals in longer sequences.

Observation 4.5. *OOD generalization implies high sharing factor, and vice versa.*

Interestingly, we observe a consistent correlation between the sharing factor κ and length generalization: cases with high sharing factor ($\kappa \gg 1$) correspond to those in which the model learns a length-generalizable solution (see Table 2). Conversely, cases with low sharing factor ($\kappa \leq 1$) are precisely those in which the learned solution fails to extrapolate beyond the training sequence lengths.

This provides additional evidence that in-distribution data efficiency and circuit sharing are fundamental implications of length generalization in state tracking.

5 CONCLUSIONS

Our study indicates that state tracking poses severe challenges for transformer-based sequence models not only out-of-distribution but also in-distribution: They require extraordinarily large amounts of training data to generalize on simple tasks and require Chain-of-Thought supervision to learn in-distribution on even moderate sequence lengths. This suggests that end-to-end learning in applied “agentic” scenarios, such as robotics or GUI control, could be even more challenging. The fact that data requirements scale with sequence length may also help explain well-known challenges at large context lengths (“context rot”).

We study performance across a limited, albeit representative, number of models and task types. Unfortunately, the large search space over parameters (performed using binary search in our experiments) requires a number of many thousand individual training runs. This makes this comparison highly computationally demanding even for the current set of models and tasks. However, as models were chosen to be simple and representative it seems very likely that the findings will persist even under slight model variations, similar to how they did in previous OOD studies.

Impact Statement This paper presents work whose goal is to advance the field of Machine Learning. There are many potential societal consequences of our work, none which we feel must be specifically highlighted here.

REFERENCES

- 486
487
488 Abbe, E., Bengio, S., Lotfi, A., Sandon, C., and Saremi, O. How far can transformers reason? the
489 globality barrier and inductive scratchpad. *Advances in Neural Information Processing Systems*,
490 37:27850–27895, 2024.
- 491 Anil, C., Wu, Y., Andreassen, A., Lewkowycz, A., Misra, V., Ramasesh, V., Slone, A., Gur-Ari, G.,
492 Dyer, E., and Neyshabur, B. Exploring length generalization in large language models. *Advances*
493 *in Neural Information Processing Systems*, 35:38546–38556, 2022a.
- 494
495 Anil, C., Wu, Y., Andreassen, A., Lewkowycz, A., Misra, V., Ramasesh, V., Slone, A., Gur-Ari, G.,
496 Dyer, E., and Neyshabur, B. Exploring length generalization in large language models. In Koyejo,
497 S., Mohamed, S., Agarwal, A., Belgrave, D., Cho, K., and Oh, A. (eds.), *Advances in Neural*
498 *Information Processing Systems*, volume 35, pp. 38546–38556. Curran Associates, Inc., 2022b.
- 499 Beck, M., Pöppel, K., Spanring, M., Auer, A., Prudnikova, O., Kopp, M., Klambauer, G., Brandstetter,
500 J., and Hochreiter, S. xlstm: Extended long short-term memory. *CoRR*, abs/2405.04517, 2024.
- 501
502 Deletang, G., Ruoss, A., Grau-Moya, J., Genewein, T., Wenliang, L. K., Catt, E., Cundy, C.,
503 Hutter, M., Legg, S., Veness, J., and Ortega, P. A. Neural networks and the chomsky hierarchy.
504 In *The Eleventh International Conference on Learning Representations*, 2023. URL <https://openreview.net/forum?id=WbxHAzkeQcn>.
- 505
506 Dummit, D. S., Foote, R. M., et al. *Abstract algebra*, volume 3. Wiley Hoboken, 2004.
- 507
508 Dziri, N., Lu, X., Sclar, M., Li, X. L., Jiang, L., Lin, B. Y., Welleck, S., West, P., Bhagavatula, C.,
509 Le Bras, R., et al. Faith and fate: Limits of transformers on compositionality. *Advances in Neural*
510 *Information Processing Systems*, 36, 2024.
- 511
512 Ebrahimi, M. and Memisevic, R. Revisiting bi-linear state transitions in recurrent neural networks.
513 In *The Thirty-ninth Annual Conference on Neural Information Processing Systems*, 2025. URL
514 <https://openreview.net/forum?id=xcqrAzYzCj>.
- 515 Ebrahimi, M., Panchal, S., and Memisevic, R. Your context is not an array: Unveiling random
516 access limitations in transformers. In *First Conference on Language Modeling*, 2024. URL
517 <https://openreview.net/forum?id=MLDlcfjUb>.
- 518
519 Fan, T.-H., Chi, T.-C., and Rudnicky, A. Advancing regular language reasoning in linear recurrent
520 neural networks. In *NAACL (Short Papers)*, pp. 45–53, 2024. URL <https://doi.org/10.18653/v1/2024.naacl-short.4>.
- 521
522 Grazi, R., Siems, J., Franke, J. K., Zela, A., Hutter, F., and Pontil, M. Unlocking state-tracking in
523 linear RNNs through negative eigenvalues. In *The Thirteenth International Conference on Learning*
524 *Representations*, 2025. URL <https://openreview.net/forum?id=UvTo3tVBk2>.
- 525
526 Hochreiter, S. and Schmidhuber, J. Long short-term memory. *Neural computation*, 9(8):1735–1780,
527 1997.
- 528 Kingma, D. P. and Ba, J. Adam: A method for stochastic optimization. *CoRR*, abs/1412.6980, 2014.
529 URL <https://api.semanticscholar.org/CorpusID:6628106>.
- 530
531 Li, B. Z., Guo, Z. C., and Andreas, J. (how) do language models track state? In *Forty-second*
532 *International Conference on Machine Learning*, 2025. URL [https://openreview.net/](https://openreview.net/forum?id=8SXosAVIFH)
533 [forum?id=8SXosAVIFH](https://openreview.net/forum?id=8SXosAVIFH).
- 534
535 Li, Z., Liu, H., Zhou, D., and Ma, T. Chain of thought empowers transformers to solve inherently
536 serial problems. In *The Twelfth International Conference on Learning Representations*, 2024. URL
537 <https://openreview.net/forum?id=3EWTEy9MTM>.
- 538
539 Liu, B., Ash, J. T., Goel, S., Krishnamurthy, A., and Zhang, C. Transformers learn shortcuts to
automata. In *The Eleventh International Conference on Learning Representations*, 2023. URL
<https://openreview.net/forum?id=De4FYqjFueZ>.

540 Merrill, W., Petty, J., and Sabharwal, A. The illusion of state in state-space models. In *International*
541 *Conference on Machine Learning*, pp. 35492–35506. PMLR, 2024.

542

543 Mitchell, T. M. *Machine learning*, volume 1. McGraw-hill New York, 1997.

544 Radford, A., Wu, J., Child, R., Luan, D., Amodei, D., Sutskever, I., et al. Language models are
545 unsupervised multitask learners. *OpenAI blog*, 1(8):9, 2019.

546

547 Sarrof, Y., Veitsman, Y., and Hahn, M. The expressive capacity of state space models: A formal
548 language perspective. In *The Thirty-eighth Annual Conference on Neural Information Processing*
549 *Systems*, 2024. URL <https://openreview.net/forum?id=eV5YIrJPdy>.

550 Terzić, M., Rahimi, A., and et al. Structured sparse transition matrices to enable state tracking in
551 state-space models. In *NeurIPS 2025*, 2025. URL [https://neurips.cc/virtual/2025/](https://neurips.cc/virtual/2025/poster/118046)
552 [poster/118046](https://neurips.cc/virtual/2025/poster/118046).

553

554 Vaswani, A., Shazeer, N., Parmar, N., Uszkoreit, J., Jones, L., Gomez, A. N., Kaiser, Ł., and
555 Polosukhin, I. Attention is all you need. *Advances in neural information processing systems*, 30,
556 2017.

557 Wen, K., Dang, X., and Lyu, K. RNNs are not transformers (yet): The key bottleneck on in-context
558 retrieval. In *The Thirteenth International Conference on Learning Representations*, 2025. URL
559 <https://openreview.net/forum?id=h3wbI8Uk1Z>.

560

561 Zhang, D. W., Defferrard, M., Rainone, C., and Memisevic, R. Grounding code understanding in step-
562 by-step execution, 2025. URL <https://openreview.net/forum?id=MUr7F193QS>.

563

564

565

566

567

568

569

570

571

572

573

574

575

576

577

578

579

580

581

582

583

584

585

586

587

588

589

590

591

592

593

A IMPLEMENTATION DETAILS

A.1 SEARCH PROCEDURE FOR DETERMINING N^*

To identify the minimal sample size N^* required for a model to successfully learn a target task, we use a hybrid Binary-Geometric search as described in Algorithm 1. The algorithm conducts a search over sample sizes, combining an initial exponential reduction phase with a subsequent binary search phase.

The search begins at a predefined maximum sample size N_{\max} . For any candidate size N , the algorithm trains models using multiple configurations drawn from a fixed hyperparameter grid Φ . In our implementation, each evaluation consists of 15 model instances (3 learning rates \times 5 random seeds). A sample size N is considered successful if at least one configuration attains validation loss below a threshold ϵ , in which case we decrease the next sample size, and otherwise, the size is labeled unsuccessful and the next trial size is increased.

Algorithm 1 Binary-Geometric Search for N^*

Inputs: Max sample size N_{\max} , Geometric Multiplier M , Step limit S , Hyperparameter grid Φ , threshold ϵ

Output: Minimal sample size N^*

```

1:  $L \leftarrow 0$  # Lower bound (largest failed size tried so far)
2:  $N^* \leftarrow N_{\max}$  # Best size so far (smallest successful size tried so far)
3:  $N \leftarrow N_{\max}$  # Current candidate
4:  $step \leftarrow 0$ 
5: while  $step < S$  do
6:   # Step 1: Evaluate model configuration at size  $N$ 
7:    $Success \leftarrow \text{false}$ 
8:   for all  $\phi \in \Phi$  do
9:      $\mathcal{L}_{\text{val}} \leftarrow$  Train and evaluate model with  $\phi$  on  $N$  samples
10:    if  $\mathcal{L}_{\text{val}} < \epsilon$  then
11:       $Success \leftarrow \text{true}$ 
12:      break
13:   # Step 2: Update bounds & choose next candidate
14:   if  $Success$  then
15:      $N^* \leftarrow N$  # Update the best value
16:     if  $L = 0$ :  $N \leftarrow N // M$  # Phase 1: Exponential decay
17:     else:  $N \leftarrow (L + N) // 2$  # Phase 2: Binary search update
18:   else
19:     if  $N = N_{\max}$  then
20:       return  $-1$  # Failure: task not learned with max sample size
21:      $L \leftarrow N$  # Update lower bound
22:      $N \leftarrow (N + N^*) // 2$  # Binary search update
23:    $step \leftarrow step + 1$ 
24: return  $N^*$ 

```

We use a geometric multiplier of $M = 1000$, a maximum of $S = 20$ search steps, and a success threshold of $\epsilon = 10^{-4}$. The hyperparameter grid is

$$\Phi = \{\text{LR} \in \{10^{-3}, 10^{-4}, 10^{-5}\}\} \times \{\text{seed} \in \{10, 20, 30, 40, 50\}\},$$

yielding 15 configurations per evaluation. Each model is trained for a fixed budget of 250k optimization steps with batch size 64 using the Adam optimizer (Kingma & Ba, 2014), independent of the training set size N . This implies a maximum feasible sample size of

$$N_{\max} = 250,000 \times 64 = 16\text{M}.$$

The maximum training set size is the minimum between the feasible 16M samples and the total number of sequences available under the specified configuration of maximum sequence length L

648 and modulus m : m^L for the *Fixed* distribution, and $\sum_{n=1}^L m^n$ for the uniform and short-to-long
649 distributions (see Section 2). The final training set size is obtained after deducting the validation set.
650

651 A.2 EVALUATION 652

653 We ensure that the training and validation sets are strictly disjoint. The validation set contains 2,000
654 samples (or at most 20% of the available data) and remains identical across different training set sizes,
655 except for variations introduced by the random seed. In addition, we always use at most 20% of the
656 available samples at each sequence length for validation, with the remainder reserved exclusively for
657 training. Also, for all tasks, multi-digit integers are represented as single tokens during tokenization.
658 Finally, for the Chain-of-Thought task format, validation loss is computed using teacher forcing
659 rather than autoregressive sampling.

660 A.3 MODELS 661

662 The transformer model is based on the GPT-2 architecture (Radford et al., 2019), with 6 layers and
663 a model (embedding/hidden) dimension of 256. Other architectural parameters, including an MLP
664 expansion factor of 4, follow the default GPT-2 (small) settings.
665

666 Both the LSTM and Dense-SSM use a single-layer recurrent cell followed by a linear classification
667 head to map the hidden state to token logits. We use an input and hidden dimension of 768 for the
668 LSTM, and 256 for the Dense-SSM. See Ebrahimi & Memisevic (2025) for additional details on
669 the Bilinear architecture used for Dense-SSM. We also experiment with a 2-layer transformer and a
670 single-layer LSTM with a hidden dimensionality of 256; sample-efficiency results for these variants
671 are provided in the Appendix Section B.3.

672 B ADDITIONAL EXPERIMENTAL RESULTS 673

674 B.1 EVALUATING LENGTH-GENERALIZATION 675

676 Table 2 reports accuracy on sequences of length $2\times$ the maximum length used during training,
677 normalized such that 0 corresponds to random chance. All models are trained using the maximum
678 available training set size for each configuration.
679
680
681
682
683
684
685
686
687
688
689
690
691
692
693
694
695
696
697
698
699
700
701

Table 2: Accuracy on sequences of length $2 \times$ the maximum used during training, normalized such that 0 corresponds to random chance.

Model	Format	Modulus	Fixed				Uniform				Short-to-Long									
			5	10	20	30	5	10	20	30	5	10	20	30						
702																				
703																				
704																				
705																				
706																				
707																				
708																				
709																				
710																				
711																				
712																				
713																				
714																				
715																				
716																				
717																				
718																				
719																				
720																				
721																				
722																				
723																				
724																				
725																				
726																				
727																				
728																				
729																				
730																				
731																				
732																				
733																				
734																				
735																				
736																				
737																				
738																				
739																				
740																				
741																				
742																				
743																				
744																				
745																				
746																				
747																				
748																				
749																				
750																				
751																				
752																				
753																				
754																				
755																				

B.2 PERMUTATION COMPOSITION TASK

Task: To show our findings generalize beyond commutative operations, we consider the task of permutation composition (simulating the symmetric group S_m). Each element of the group represents a permutation of the set $\{1, \dots, m\}$, resulting in a group of cardinality $|S_m| = m!$. In our experimental setup, each permutation $\pi \in S_m$ is bijectively mapped to a unique integer token in $\{0, 1, \dots, m! - 1\}$. Given an input sequence of n permutations $\mathbf{x} = (\pi_1, \pi_2, \dots, \pi_n)$, the model is required to compute their sequential composition:

$$y = \pi_n \circ \pi_{n-1} \circ \dots \circ \pi_1, \tag{5}$$

where \circ denotes the permutation composition operator. This task significantly elevates the complexity of state tracking, as the model can no longer rely on the order-invariance property characteristic of abelian groups.

Algebraic Significance: The symmetric group S_m serves as the canonical non-commutative structure for evaluating state tracking. Its fundamental importance is grounded in *Cayley's Theorem*, which states that every finite group G is isomorphic to a subgroup of the symmetric group $S_{|G|}$ (Dummit et al., 2004). Hence, by analyzing performance on S_m , we effectively probe the model's capacity to internalize the transition dynamics of any finite discrete group.

As noted in Figure 7, we observe the same patterns described in Section 4 and Figure 6, supporting the generalization of these findings and the subsequent arguments to non-commutative state-tracking tasks.

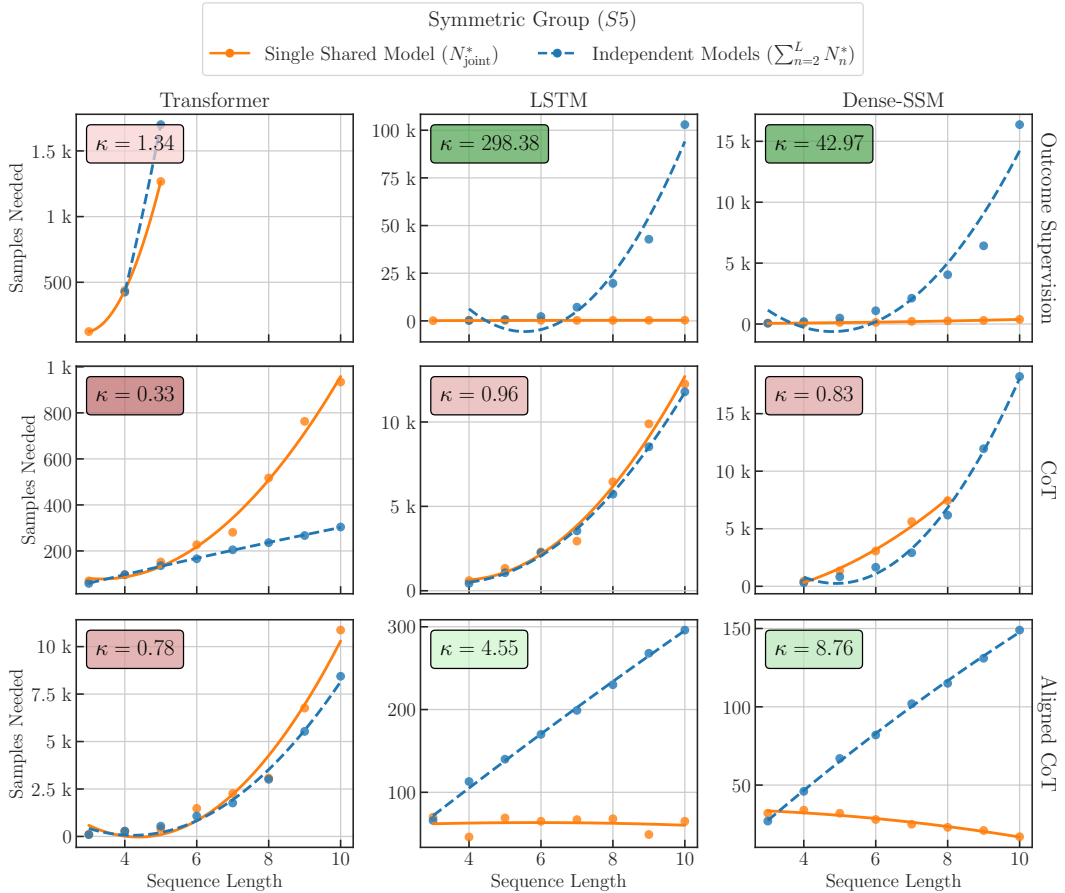


Figure 7: Similar to Figure 6, but for permutation composition task. The results suggest that transformers learn largely isolated solutions for each sequence length.

B.3 DATA EFFICIENCY EVALUATION FOR SMALLER MODELS

Table 3: N^* for LSTMs with 256 and 768 hidden dimensions. We observe similar trends across both model sizes.

Model	Format	Mod.	Fixed				Uniform				Short-to-Long			
			5	10	20	30	5	10	20	30	5	10	20	30
LSTM Dim = 256	Outcome Supervision	2	14	202	257	413	26	34	67	109	12	13	26	16
		3	151	620	-	-	84	122	317	686	81	180	132	178
		5	1.3K	6.7K	-	-	487	876	-	-	788	1.4K	-	-
		10	6.3K	-	-	-	3.4K	-	-	-	5.1K	-	-	-
		15	21.9K	-	-	-	11.1K	-	-	-	-	-	-	-
		20	-	-	-	-	-	-	-	-	-	-	-	-
		50	-	-	-	-	-	-	-	-	-	-	-	-
		75	-	-	-	-	-	-	-	-	-	-	-	-
		100	-	-	-	-	-	-	-	-	-	-	-	-
		LSTM Dim = 256	CoT	2	26	346	3.2K	14.9K	-	853	24.6K	306.4K	-	920
3	-			5K	20.5K	-	-	12.2K	129.2K	-	-	29.9K	-	-
5	-			9.6K	32K	-	-	26.3K	68.1K	-	-	2.5M	-	-
10	10.4K			14.8K	15.4M	-	21.7K	53.1K	-	-	21.6K	-	-	-
15	19.3K			21.1K	-	-	46.3K	162.1K	-	-	73.7K	-	-	-
20	30.9K			21.6K	-	-	64.6K	351.8K	-	-	276.7K	-	-	-
50	33.7K			36.5K	-	-	413.8K	14.7M	-	-	8.4M	-	-	-
75	41.1K			50.5K	-	-	595.1K	-	-	-	-	-	-	-
100	46.4K			13.4M	-	-	3.8M	-	-	-	-	-	-	-
LSTM Dim = 256	Aligned CoT			2	8	8	10	8	4	8	2	8	12	7
		3	10	11	8	8	21	17	8	8	27	32	39	39
		5	95	75	52	39	144	101	70	54	142	148	225	209
		10	324	227	205	209	477	379	317	257	606	1.2K	1.7K	1.9K
		15	543	502	452	467	846	677	637	772	1.4K	4K	8.4K	57.6K
		20	993	902	919	1K	1.2K	1.3K	1.2K	1.2K	2.6K	10.1K	176.3K	194.9K
		50	4.6K	5.3K	7.3K	4K	5.8K	7.3K	8.7K	11.5K	20K	168.2K	-	-
		75	9.2K	9.2K	13.5K	15.4K	10.3K	12.2K	15.7K	20K	42.6K	1.2M	-	-
		100	14.5K	15.6K	19.8K	32.6K	16K	23.9K	25.3K	9.1M	78.6K	-	-	-
		LSTM Dim = 768	Outcome Supervision	2	14	101	252	309	16	21	64	54	12	9
3	195			620	1.7K	-	78	122	317	526	83	90	90	100
5	2K			5.9K	-	-	387	707	-	-	381	22.7K	-	-
10	6.4K			-	-	-	2.2K	8.6K	-	-	2.2K	-	-	-
15	18.8K			-	-	-	11.8K	-	-	-	-	-	-	-
20	-			-	-	-	-	-	-	-	-	-	-	-
50	-			-	-	-	-	-	-	-	-	-	-	-
75	-			-	-	-	-	-	-	-	-	-	-	-
100	-			-	-	-	-	-	-	-	-	-	-	-
LSTM Dim = 768	CoT			2	20	307	4.7K	8.6K	45	692	13.4K	37.1K	48	843
		3	-	2.9K	9.3K	14K	-	7.4K	40.3K	5.2M	-	29K	-	-
		5	1.6K	10.3K	20.4K	44K	2K	28.4K	68.1K	2.1M	2.1K	-	-	-
		10	6.1K	15.7K	29.1K	-	14.3K	544.4K	500K	-	16.8K	-	-	-
		15	15.8K	21.1K	42K	-	32K	67K	-	-	65.6K	-	-	-
		20	21.2K	29.6K	54.3K	-	40.7K	409.1K	14M	-	215.4K	-	-	-
		50	43K	50.4K	-	-	206K	2.2M	-	-	10.4M	-	-	-
		75	56.5K	58K	-	-	4M	-	-	-	-	-	-	-
		100	84.2K	9.5M	-	-	-	-	-	-	-	-	-	-
		LSTM Dim = 768	Aligned CoT	2	4	6	2	2	4	4	2	2	9	7
3	10			8	8	6	18	12	6	8	27	28	34	34
5	95			70	39	31	153	107	80	47	142	148	253	235
10	278			194	146	130	447	313	247	232	685	1.3K	1.8K	2K
15	534			478	409	371	865	631	567	500	1.5K	3.9K	5.2K	7.1K
20	798			672	652	798	1.3K	934	870	820	2.7K	9.4K	13.4K	25.9K
50	3.7K			4.6K	6K	7.4K	4.1K	5.3K	6.1K	6.9K	14.7K	156.2K	-	-
75	7.4K			9.2K	12.2K	13.3K	8.4K	11.3K	14.2K	16.8K	41.1K	697.4K	-	-
100	12.8K			16.6K	21.9K	23.7K	13.3K	19.4K	24.3K	28.5K	99.7K	-	-	-

Table 4: N^* for transformers with 2 and 6 layers. We observe similar trends across both model depths.

Model	Format	Modulus	Fixed				Uniform				Short-to-Long			
			5	10	20	30	5	10	20	30	5	10	20	30
Transformer 2 Layers	Outcome Supervision	2	-	594	-	-	48	807	-	-	48	971	-	-
		3	134	-	-	-	-	-	-	-	-	-	-	
		5	1.5K	-	-	-	1.7K	-	-	-	-	-	-	
		10	-	-	-	-	-	-	-	-	-	-	-	
		15	-	-	-	-	-	-	-	-	-	-	-	
		20	-	-	-	-	-	-	-	-	-	-	-	
		50	-	-	-	-	-	-	-	-	-	-	-	
		75	-	-	-	-	-	-	-	-	-	-	-	
		100	-	-	-	-	-	-	-	-	-	-	-	
		Transformer 2 Layers	CoT	2	14	26	21	23	37	214	724	1.1K	42	824
3	19			24	25	31	93	456	1.3K	1.7K	117	28.8K	-	-
5	32			31	34	39	241	893	1.8K	2K	653	2.4M	-	-
10	86			61	52	54	600	1.8K	3.6K	4.1K	11.1K	-	-	
15	160			97	79	62	805	2.9K	7.4K	6.8K	54.2K	-	-	
20	229			142	97	78	1.3K	3K	8.5K	10K	168.8K	-	-	
50	795			542	334	272	3.2K	6.2K	-	16M	6.5M	-	-	
75	1.5K			958	688	600	5.1K	15.1K	70.8K	-	-	-	-	
100	2.1K			1.5K	1.1K	1K	6.8K	20.3K	33.6K	209.2K	-	-	-	
Transformer 2 Layers	Aligned CoT			2	26	197	3K	2K	37	439	5.2K	363.8K	36	869
		3	129	2.1K	7.5K	-	239	11.1K	-	-	234	29.9K	-	-
		5	1.1K	6.5K	-	-	1.6K	40.9K	-	-	1.5K	2.5M	-	-
		10	2.1K	12.4K	-	-	4.6K	156.1K	-	-	11.9K	-	-	-
		15	3.1K	31.2K	-	-	8.2K	1.6M	-	-	55.3K	-	-	-
		20	4.2K	59.5K	-	-	11.2K	-	-	-	175.5K	-	-	-
		50	10.1K	-	-	-	15.8K	-	-	-	6.8M	-	-	-
		75	21.6K	-	-	-	33.8K	-	-	-	-	-	-	-
		100	25K	-	-	-	99.8K	-	-	-	-	-	-	-
		Transformer 6 Layers	Outcome Supervision	2	19	364	-	-	37	549	-	-	45	913
3	119			-	-	-	-	-	-	-	243	-	-	-
5	1.1K			-	-	-	2.6K	-	-	-	1.5K	-	-	-
10	-			-	-	-	-	-	-	-	-	-	-	-
15	-			-	-	-	-	-	-	-	-	-	-	-
20	-			-	-	-	-	-	-	-	-	-	-	-
50	-			-	-	-	-	-	-	-	-	-	-	-
75	-			-	-	-	-	-	-	-	-	-	-	-
100	-			-	-	-	-	-	-	-	-	-	-	-
Transformer 6 Layers	CoT			2	10	16	19	20	36	198	744	1K	39	824
		3	16	18	21	25	78	465	1.2K	1.4K	108	28.8K	-	-
		5	33	30	31	34	148	1.1K	1.7K	1.7K	647	2.4M	-	-
		10	94	66	62	70	427	2.3K	3.4K	4K	11K	-	-	
		15	166	116	78	107	709	2.5K	5K	5.1K	54.3K	-	-	
		20	377	178	116	135	1K	3.8K	5.6K	7.4K	168.6K	-	-	
		50	1.1K	678	553	470	2.6K	8.6K	12K	11.2K	6.4M	-	-	
		75	1.7K	1.2K	1K	946	4.2K	11K	18.1K	16.1K	-	-	-	
		100	2.5K	1.9K	1.6K	1.6K	5.8K	13.2K	21.1K	19.1K	-	-	-	
		Transformer 6 Layers	Aligned CoT	2	16	121	644	1.2K	27	313	2K	11.7K	19	856
3	91			2K	3.7K	4K	180	8.3K	66.8K	-	207	29.7K	-	-
5	528			3.9K	9.2K	20.8K	671	14.5K	2M	-	909	2.4M	-	-
10	1.3K			6K	15.5K	131.4K	1.7K	32.3K	-	-	11.2K	-	-	-
15	1.5K			7.9K	23.3K	-	2.4K	61.5K	-	-	55K	-	-	-
20	2.6K			21.9K	85.3K	-	4.5K	190.9K	-	-	172.6K	-	-	-
50	13K			1M	-	-	22K	-	-	-	6.7M	-	-	-
75	21.1K			15.2M	-	-	102.1K	-	-	-	-	-	-	-
100	23.6K			-	-	-	8M	-	-	-	-	-	-	-